Polym. Bull. (2012) 68:1801–1813
DOI 10.1007/s00289-011-0648-z

ORIGINAL PAPER

Electrochemical synthesis of poly(3′-alkyl-terthiophenes). Characterization and applications

Fernando R. Díaz · Ignacio Jessop ·
Christian Núñez · M. Angélica del Valle ·
Pedro Pablo Zamora · Jean Christian Bernède

Received: 10 January 2011 / Revised: 9 July 2011 / Accepted: 7 October 2011 /

Abstract A new series of polymers obtained from 3′-alkyl-terthiophene monomers have been electropolymerized aimed at using them as raw materials for the development of electronic devices, e.g., solar cell and organic light-emitting diodes, among others. The polymers were characterized by infrared and UV–Vis spectroscopy and cyclic voltammetry. Cyclic voltammetry results revealed that during polymerization both terthiophene system and substituent groups are oxidized, but these processes are reversible. The products were tested in solar cells and the maximum yield obtained was 0.01%.

Keywords Conductive polymers · Substituted terthiophenes · Electrochemical polymerization · Photoelectronic devices

Introduction

During the last few decades, semiconductive polymers have revolutionized materials world by providing the evolution of a novel generation of a number of optical and electronic devices. Among these polythiophene (PT) materials stand out because, among other features, they exhibit thermal and environmental stability, good solubility, and high conductivity when doped. These PTs have been utilized in a variety of applications, e.g., transistors, hole-injection layers LED devices, electrical conductors, environmental sensors, and photovoltaic cells are worth mentioning [1]. The PTs are attractive candidates for the design of new photovoltaic

---

F. R. Díaz · I. Jessop (✉) · C. Núñez · M. A. del Valle · P. P. Zamora
Facultad de Química, Pontificia Universidad Católica de Chile, Vicuña Mackenna,
4860 Santiago, Chile
e-mail: iajessop@uc.cl

J. C. Bernède
UNAM, Ajou Moltech, UMR 6200, 2 rue de la Houssinière, BP 92208, 44000 Nantes, France

devices because is relatively easy to incorporate a wide variety of substituent moieties to the main chain, increasing the range of photon absorption and favoring exciton dissociation [2]. It was found that the use of terthiophenes (TThs) as PTs precursors led to improved photovoltaic efficiency of cells prepared from them, as compared to devices based on PTs synthesized from 3-methylthiophene or bithiophene [3]. The reason for this difference is presumably associated to the ability of polyterthiophenes (PTThs) to adopt a more ordered 3D structure due to the pre-existing order in the monomer [4]. On the other hand, the high stability conferred by the aromatic system to the radical cation originated during TThs oxidation process brings about a decrease of the potential required to start its oxidation as compared to the potential needed to initiate Ths electro-polymerization, reducing thus the probability of polymer overoxidation [5].

The electro-generation of polymer layers represents a great advantage in the synthesis of conductive polymers as a feasible alternative to chemical coupling of di-bromoderivatives or chemical oxidation with $FeCl_3$. The product is obtained directly on the electrode surface and control of the whole process is possible since the polymer generation proceeds by applying a precisely controlled potential [6]. Besides, electrosynthesis allows the morphology of the deposit to be controlled, which is essential when designing materials for the development of electronic devices.

Consequently, our work was focused on the electrochemical synthesis of semiconducting polymers based on new 3′-alkyl-terthiphene monomers modified with aromatic groups that will confer a new ordering and spacing to the polymer chains. These polymers have been designed for their prospective use in photoelectronic devices, e.g., light-emitting diodes and/or solar cells.

Experimental

All solvents and reagents used in this investigation were purchased from Aldrich and used as received. NMR spectra were recorded on a 200 MHz Bruker spectrometer. FT-IR monomers and polymers spectra were recorded on a Vector 22 Bruker spectrometer using pressed KBr pellets. Microanalysis was carried out on a Fisons Analizer, Model EA-1108. UV–Visible spectra were recorded on an Analitik Jena spectrophotometer, model SPECORD 40, using a 1 cm optical path quartz cells. Electrochemical studies were accomplished on a BAS 50 W Voltametric Analyzer using a three-compartment cell. A platinum disc, a platinum foil and a partially etched SnO_2-coated glass (conducting glass) of, respectively, 0.07, 4, and 2 cm^2 geometric area were employed as working electrode. Ag/AgCl, KCl (sat'd) was used as reference electrode, while a platinum wire of large geometric area was used as counter-electrode. Monomer concentration was 1×10^{-3} M and Tetrabutylammonium hexafluorophosphate TBAHFP in dichloromethane (1×10^{-2} M) was the supporting electrolyte. Prior to each measurement the working solution was deaerated by flushing with high-purity argon for 15–20 min and then an argon atmosphere was maintained over the solution throughout the experiment. Polymer samples prepared on conductive glass were sent to Nantes University, France, where the properties of cells prepared from them were evaluated using a device consisting of a Kethley 617 programmable Electrometer, a Kethley 2000 Multimeter, and a Lambda IEEE-488 programmable power supply, Model LLS6060-GPIB.

Monomers synthesis

The precursors synthesis was conducted in several steps, Fig. 1. For 3-(6-bromohexyl)thiophene formation and substitution of the terminal halogen in the alkyl chain by the aromatic system, the route described by Bäuerle et al. [7] was chosen. $3'$-Alkyl-terthiophenes preparation was accomplished utilizing Kumada cross-coupling reaction [8].

General procedure for TThs synthesis

To a solution containing 1.5 g (3.2 mmol) 2.5-dibromo-3-[6-(aryl)-hexyl]thiophene, 0.1 g (0.18 mmol) Ni(dppp)Cl$_2$ and 100 mL of anhydrous diethyl ether, 1.2 g (6.4 mmol) 2-bromomagnesium-thiophene was added and refluxed for 24 h. The system was cooled to room temperature and the resulting mixture poured into 100 mL of 5% HCl solution. The organic phase was washed with distilled water, dried with MgSO$_4$ and vacuum concentrated. The product was separated by column chromatography, using silica gel as support and petroleum ether as eluent, followed by crystallization from isopropyl alcohol. All products were characterized by ^{1}H NMR, ^{13}C NMR, and FT-IR. The results are presented below:

$3'$-[6-(Naphthalene-2-yloxy)-hexyl]-$[2.2':5.2'']$terthiophene (TTh-I): Yellow solid, yield 1.38 g (91%), MP 75–76 °C, 1H NMR (CDCl$_3$) $\delta = 1.57$ (m, 4H), 1.76 (m, 2H), 1.90 (m, 2H), 2.81 (t, 2 H, $J = 7.3$ Hz), 4.10 (t, 2H, $J = 6.4$ Hz), 7.03 (dd, 1H, $J = 5.1$ and 3.6 Hz), 7.03 (s, 1H), 7.06 (dd, 1H, $J = 5.0$ and 3.6 Hz), 7.12 (dd, 1H, $J = 3.6$ and 1.1 Hz), 7.14 (m, 1H), 7.15 (dd, 1H, $J = 3.6$ and 1.1 Hz), 7.17 (m, 1H), 7.21 (dd, 1H, $J = 5.1$ and 1.1 Hz), 7.30 (dd, 1H, $J = 5.1$ and 1.1 Hz), 7.32 (m, 1H), 7.43 (m, 1H), and 7.74 (m, 3H). 13C NMR (CDCl$_3$) $\delta = 26.0$, 29.24, 29.28, 30.5, 67.9, 77.3, 106.7, 119.0, 123.5, 123.6, 124.4, 125.4, 126.0, 126.3, 126.5, 126.7, 127.5, 127.7, 127.9, 128.9, 129.3, 134.7, 135.3, 135.9, 137.2, 140.1, 157.1. FT-IR (KBr, cm^{-1}) 816 (γ C–H 2,3, 5-trisubstituted thiophenes), 1.017 (ν C–O), 1.258 (ν C–O-C), 1.463 (ν PhC-C), 2.856 y 2.934 (ν C–H of alkyl chain), 3.062 y 3.105 (v ThC-H). Elemental analysis for C$_{28}$H$_{26}$OS$_3$. Calcd.: C, 70.85%, H, 5.52, S, 20.26%. Found: C, 70.82%, H, 5.49%, S, 20.24%.

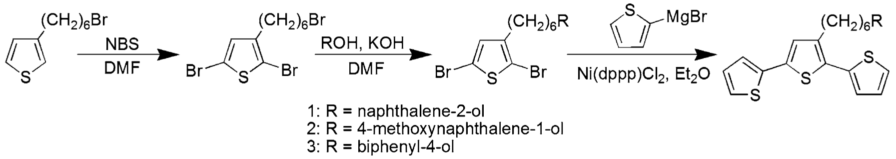

Fig. 1 Monomers preparation scheme

3′-[6-(4-Methoxynaphthalene-1-yloxy)-hexyl]-[2.2′:5.2″]terthiophene (TTh-II): Yellow solid, yield 1.51 g (93%), MP 36–38 °C, 1H NMR ($CDCl_3$) $\delta = 1.58$ (m, 6H), 1.92 (t, 2H, $J = 6.0$ Hz), 2.77 (t, 2H, $J = 8.0$ Hz), 3.96 (s, 3H), 4.08 (t, 2H, $J = 6.0$ Hz), 6.69 (s, 2H), 7.03 (dd, 1H, $J = 5.0$ and 3.6 Hz), 7.03 (s, 1H), 7.08 (dd, 1H, $J = 5.0$ and 3.6 Hz), 7.10 (dd, 1H, $J = 3.5$ and 1.0 Hz), 7.15 (dd, 1H, $J = 3.5$ and 1.0 Hz), 7.20 (dd, 1H, $J = 5.0$ and 1.1 Hz), 7.26 (dd, 1H, $J = 5.0$ and 1.0 Hz), 7.52 (m, 2H), 8.21 (m, 2H). 13C NMR ($CDCl_3$) $\delta = 26.1$, 29.3 (2C), 30.5 (2C), 55.7, 68.3, 103.2, 104.1, 121.7, 121.8, 123.6, 124.3, 125.4, 125.7 (3C), 126.4 (3C), 127.4, 127.8, 129.7, 135.3, 135.9, 137.2, 140.1, 149.0, 149.4. FT-IR (KBr, cm^{-1}) 819 (γ CH 2,3,5-trisubstituted thiophenes), 1.023 (ν CO), 1.271 (ν AlkC-O-PhC), 1.460 (ν PhC-C), 2.853 and 2.930 (ν CH of alkyl chain), 3.071 and 3.104 (v ThC-H). Elemental analysis for $C_{29}H_{28}O_2S_3$. Calcd.: C, 69.01%, H, 5.59%, S, 19.06%. Found: C, 68.98%, H 5.56%, S, 19.02%.

3′-[6-(Biphenyl-4-yloxy)-hexyl]-[2.2′:5.2″]terthiophene (TTh-III): Yellow solid, yield 1.17 g (73%) MP 99–101 °C, 1H NMR ($CDCl_3$) $\delta = 1.50$ (m, 4H), 1.74 (m, 4H), 2.79 (t, 2H, $J = 8.0$ Hz), 4.01 (t, 2H, $J = 6.0$ Hz), 6.97 (m, 2H), 7.01 (dd, 1H, $J = 5.1$ and 3.6 Hz), 7.05 (s, 1H), 7.09 (dd, 1H, $J = 5.0$ and 3.6 Hz), 7.11 (dd, 1H, $J = 3.6$ and 1.1 Hz), 7.16 (dd, 1H, $J = 3.6$ and 1.1 Hz), 7.21 (dd, 1H, $J = 5.1$ and 1.1 Hz), 7.26 (m, 1H), 7.32 (dd, 1H, $J = 5.1$ and 1.1 Hz), 7.41 (m, 2H), 7.57 (m, 4H), 13C NMR ($CDCl_3$) $\delta = 25.9$, 29.2 (2C), 29.7, 30.5, 67.9, 114.6 (2C), 123.6, 124.4, 125.4, 126.5, 126.6 (2C), 126.7 (2C), 127.5 (2C), 127.9, 128.1, 128.7, 129.6, 133.5, 135.2, 137.2, 140.0, 140.9, 158.7. FT-IR (KBr, cm-1) 825 (γ CH 2,3,5-trisubstituted thiophenes), 1.043 (ν C–O), 1.269 (ν AlkC-O-PhC), 1.487 (ν PhC-C), 2.855 and 2.927 (ν CH of the alkyl chain), 3.030 and 3.105 (v ThC-H). Elemental analysis for $C_{30}H_{28}OS_3$. Calcd.: C, 71.96%, H 5.64%, S, 19.21%. Found: C, 71.93%, H 5.61%, S, 19.18%.

Results and discussions

Electrochemical polymerization

Figure 2 shows the i/V transient of TTh-I, TTh-II, and TTh-III monomeric units obtained by successive voltammetric scans at 0.1 V s^{-1} within the optimal potential range established for each case.

More than one oxidation process was observed for each monomer during the first cycle. The first peak, between 0.7 and 0.9 V, corresponds to monomer oxidation to its radical cation. The following peaks might be related to the coupling of two radical cations to produce a dication, which becomes a dimer after the loss of two protons and re-aromatization [9, 10], and to the doping that occurs simultaneously during oligomerization and further polymerization processes. Moreover, the oxidation proceeds and the voltammogram exhibits a current loop, suggesting an electrode surface modification. The undoping process is the main responsible for the cathodic peak.

The voltammetric profiles also showed that the anodic current increases and the cathodic current decreases as the number of cycles raises, accounting for the

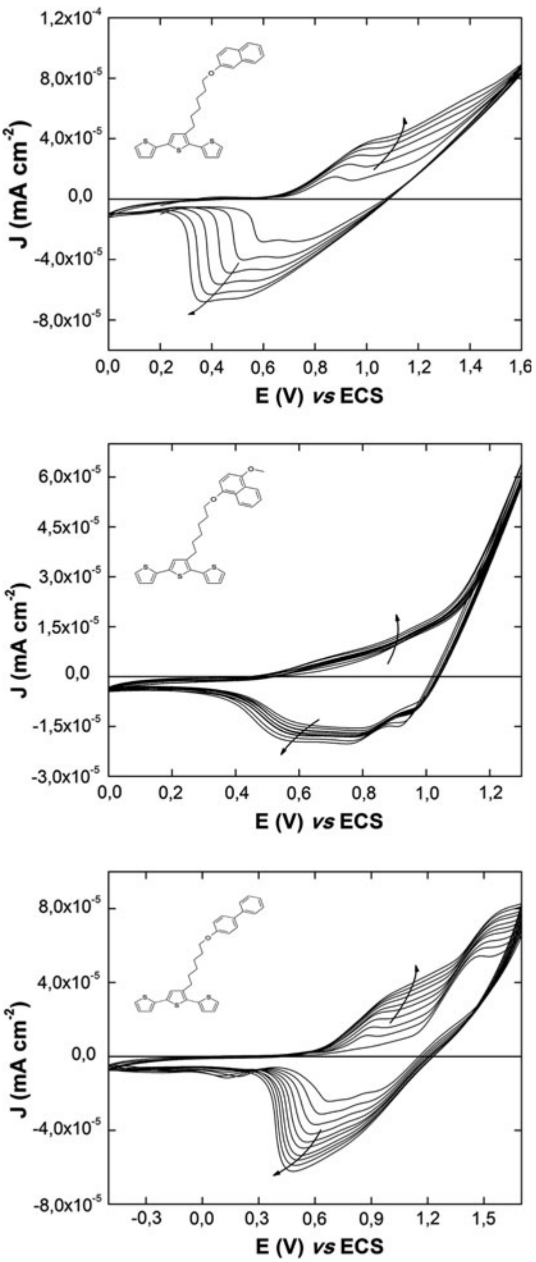

Fig. 2 Voltammetric profiles of TTh-I, TTh-II, and TTh-III monomers. Interface: Pt | 1.0×10^{-3} M + 1.0×10^{-2} M TBAHFP, CH_2Cl_2, $v = 100$ mV s^{-1}

formation of a polymeric film on the electrode surface. Moreover, as the number of cycles increases the oxidation onset potential shifts toward more anodic values. This finding indicates that oxidation becomes more difficult as chain length increases, which can be ascribed to the presence of a bulky substituent group that prevents easy ordering of the polymer to continue growing.

Moreover, in order to have at our disposal a standard to compare the electrochemical results obtained for the monomers under survey, non-substituted TTh electro-polymerization was conducted under the same working conditions. It was found that TTh oxidation potential is higher than for substituted monomers. This outcome could be explained by considering that the alkyl chain provides electron density to the TTh aromatic system that would help to stabilize the generated radical cation. On the other hand, the initial oxidation potential for unsubstituted TTH shifts toward lower values as a function of the number of cycles, in contrast to what happens with substituted monomers. This fact would support the assumption that the bulky substituent group generates a negative effect in the ordering of the polymer deposited upon the electrode surface.

The response of the prepared polymers, Fig. 3, was assessed by immersing the modified electrode in a solution containing just supporting electrolyte. An oxidation and reduction wave can be observed for PTTh-I, PTTh-II, and PTTh-III, respectively, with current peaks at potentials that validate the abovementioned assignment, (Fig. 2), of these processes occurring simultaneously during electro-polymerization. The voltammetric profiles are rapidly stabilized without observing a significant signal change, despite of continuous and successive repetition of the perturbation, suggesting the polymeric deposits undergo neither degradation nor decomposition during the process. Furthermore, a color change of the deposits, associated to an increase or decrease in the length of the conjugated chain, was observed. This outcome arises because the redox process generates a rearrangement of Th rings leading to a change in polymer planarity and, accordingly, to absorption modification (electrochromism phenomenon).

Because the electrosynthesis of polymers from monomers possessing substituent groups amenable to be oxidized presented the disadvantage of modifying these groups, the voltammetric behavior of the substituent molecules was studied under the same experimental conditions used for monomers electro-oxidation (Fig. 4). The results revealed that all substituent groups underwent totally reversible oxidation within the working potential range. The observed current demonstrated that the substituent group exerted little influence on the polymeric unit. The alkyl chain length and the ether group that confer greater mobility, enable a suitable rearrangement of the substituent group during polymerization. The alkyl chain also allows the aromatic rings in the substituent of the TTh system to be moved apart, precluding conjugation between them. The redox process of the substituent, along with doping–undoping process, was evidenced in the PTThs survey, except for PTTh-III. This fact, that could be considered a negative feature of the products, can be used in other applications in which, for example, favorable or unfavorable coordinating capacity of the polymer is required.

FT-IR spectroscopy

To corroborate the structure of deposited polymers onto conductive glass, a FTIR-ATS study was accomplished. The results are presented in Table 1.

The absence of thiophene C–H(α) stretching at about 3100 cm^{-1} must be underlined. This finding indicates the polymerization takes place mainly at C(2) and

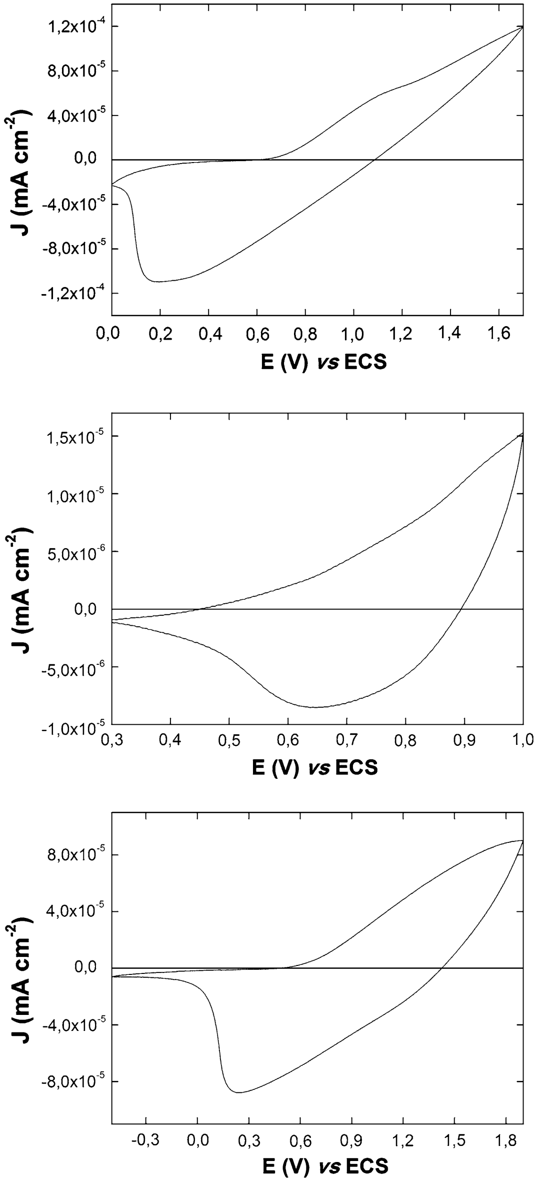

Fig. 3 Response of PTTh-I, PTTh-II, and PTTh-III polymers during electrochemical doping and undoping

C(5) of the ring. This was verified by the signals found at around 835 and 800 cm^{-1} which are characteristics of 2,5-disubstituted thiophenes.

The low solubility of the products in typical organic solvents precluded running NMR spectra, but infrared studies proved the obtained polymers were those expected.

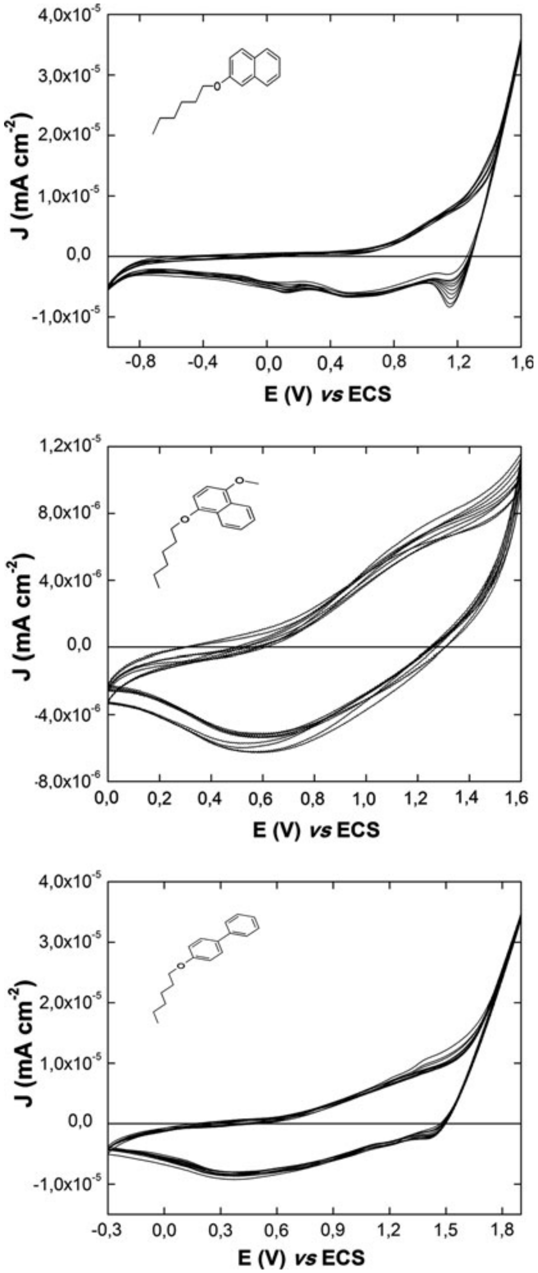

Fig. 4 i/V transient of the substituent groups S-I, S-II, and S-III. Interface: Pt | 1.0×10^{-3} M + 1.0×10^{-2} M TBAHFP, CH_2Cl_2, $v = 100$ mV s^{-1}

UV–Vis spectroscopy

Figure 5 shows UV–Vis spectra of polymers in their neutral and doped state obtained on conducting glass.

Table 1 Assignment of the main frequencies (cm^{-1}) found for the studied polymers deposited on conductive glass

PTTh-I	PTTh-II	PTTh-III	Assignment
3063	3079	3063	Stretching CH (β) of thiophene
2934	2925	2934	CH_2 asymmetric stretching of the alkyl chain
2858	2852	2857	CH_2 symmetric stretching of the alkyl chain
1599	1594	1609	Stretching of ortho-disubstituted aromatic ring
1259	1259	1244	C–O–C stretching
835	868	831	CH oop bending in 2,3,5-trisubstituted thiophenes
806	796	796	CH oop bending of 2,5-disubstituted thiophenes

The maximum absorption of these polymers in their neutral state between 420 and 490 nm was assigned to π–π^* transitions of thiophene chains. A second peak between 750 and 785 nm corresponds to a radical bication formation [9]. For doped polymers, this peak showed a slight shift toward the red region. It is noteworthy to mention that at the first maximum the polymers are red-colored, while at the second one they are blue-colored. Doped polymers spectra also presented an absorption band at around 1.000 nm that was assigned to another low-energy transition in the oxidized state, presumably due to the presence of substituent groups.

Electrical conductivity

Conductivity determined for electro-synthesized polymers and unsubstituted PTTh in their doped and undoped state are included in Table 2.

These results suggest the materials are situated in the semiconductor range of conductivity. Poly(3′-alkyl-terthiophenes) conductivity values are significantly lower than that for the reference PTTh. This difference can be ascribed to the degree of chains disorder due to steric effect induced by bulky substituents.

PTThs assessment for photocell fabrication

The monomers were chosen in such a way that after polymerization they displayed a dual behavior, i.e., the PTh chains should be capable of hole transport while the fused ring system of the substituents should present adequate electron conduction. However, electrochemical studies revealed these materials were mainly positively doped. Consequently, for photovoltaic devices fabrication the different polymers were used as electron donor materials while perylene was the electron acceptor material.

Figure 6 shows the *I*–*V* characteristic of photovoltaic cells prepared from PTTh-I and PTTh-III. PTTh-II showed no response to this test.

Usually four parameters are assessed for the characterization of photovoltaic cells, namely, J_{sc} (short circuit current density), V_{oc} (open circuit voltage), FF (fill factor), and η (photocell efficiency). Obtained parameters values are listed in Table 3.

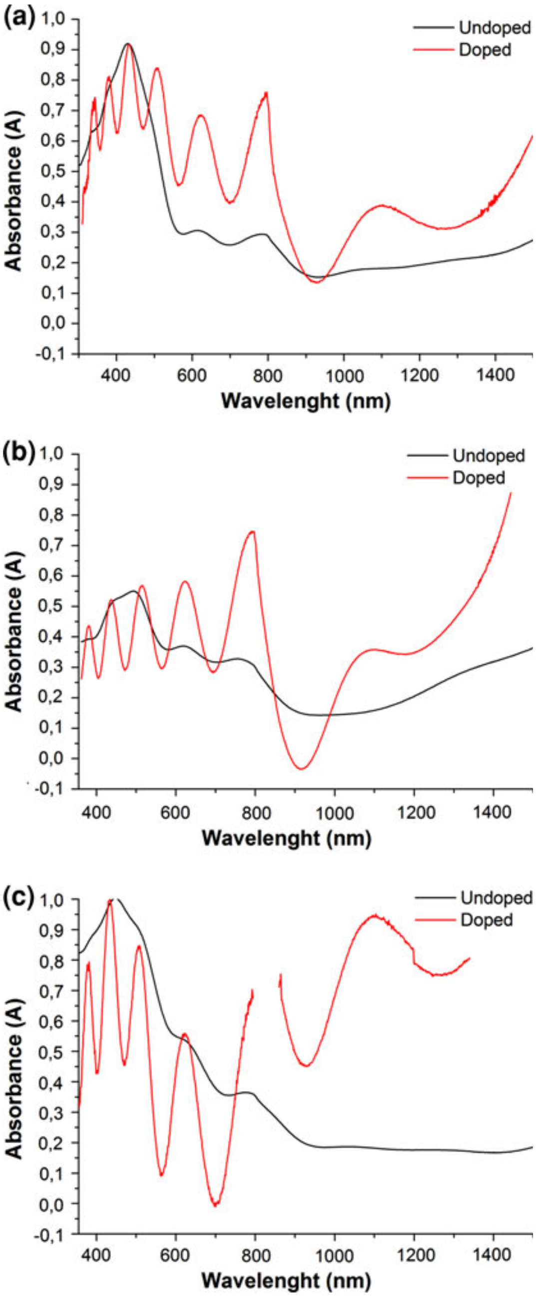

Fig. 5 PTTh-I (a), PTTh-II (b), and PTTh-III (c) UV–Vis spectra of deposits in their neutral and doped state on conductive glass

The equivalent circuit commonly used to interpret the characteristics of solar cells consists of a current photogenerator connected in parallel with a diode, which represents the *I*–*V* characteristic under dark conditions, while parasitic series and shunt resistances are represented by R_s and R_{sh}, respectively. The slopes at the short

Table 2 Poly(3′-alkyl-terthiophenes) and PTTh electrical conductivity in their doped and undoped state

Polymer	Undoped (S cm^{-1})	Doped (S cm^{-1})
PTTh-I	2.0×10^{-9}	3.0×10^{-5}
PTTh-II	6.2×10^{-8}	8.5×10^{-6}
PTTh-III	3.0×10^{-9}	1.0×10^{-5}
PTTh	6.7×10^{-7}	4.3×10^{-3}

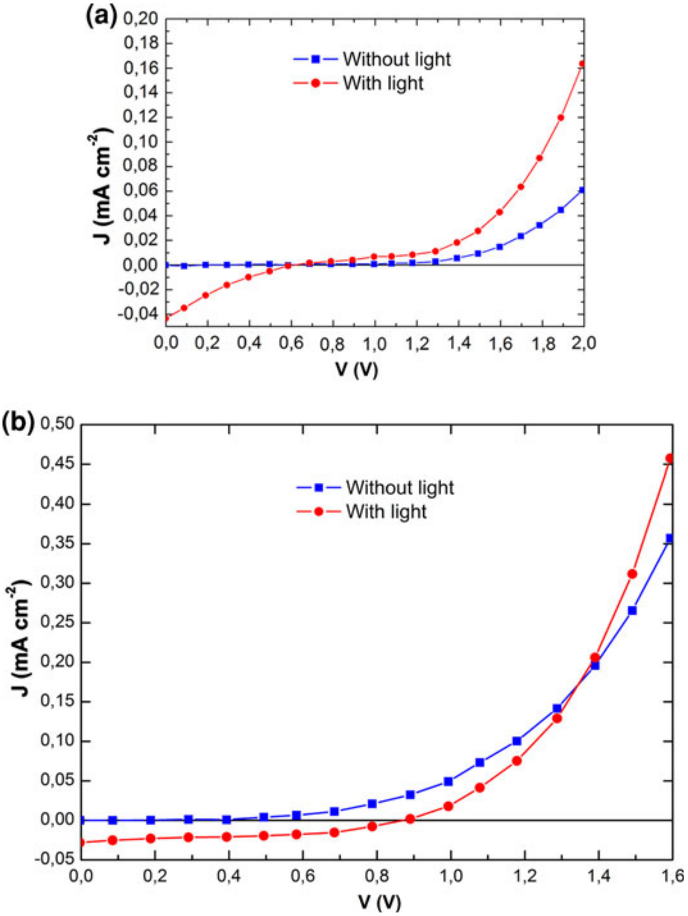

Fig. 6 *I*–*V* characteristics of photocells prepared from polymers PTTh-I (a) and PTTh-III (b) in the presence and absence of light

circuit point and at the open circuit voltage of the electrical cells characteristics are the inverse values of the shunt resistance (R_{sh}) and the series resistance (R_s) of the equivalent circuit scheme of a solar cell, respectively [11]. It can be seen from Fig. 6 that cells using PTTh-III as electron donor exhibit higher shunt resistance and smaller series resistance than the one using PTTh-I. This justifies the higher V_{oc} and

Table 3 Photocell electrical parameters

Polymer	J_{sc} (mA cm^{-2})	V_{oc} (V)	FF	η
PTTh-I	0.043	0.61	0.27	0.007
PTTh-III	0.028	0.87	0.41	0.010

FF of the former cells. Indeed, V_{oc} decrease may arise from pinholes that short circuit the PV cell and decrease R_{sh}. Also, the difference in voltage could be ascribed to the nature of the substituent group. FF depends strongly on the band structure matching which means that cells using PTTh-III as electron donor present better contact with the anode [12]. However, J_{sc} is higher when PTTh-I is utilized as electron donor, which could be attributed to its higher conductivity.

As far as the efficiency of cells prepared from monomers is concerned, it is noteworthy that the photocell designed from PTTh-III gave better results, however, this value is much lower than that obtained with other organic systems [13, 14]. Although these results were not the expected ones, we still believe that our monomers can be used as electron donor in the fabrication of interpenetrating network photocells.

Conclusions

Electrochemical synthesis of polymers derived from new substituted TTh was accomplished upsetting neither the monomeric structure of the TTh system nor the oxidation-sensitive substituent group. Infrared experimental results enabled us to infer that during the electro-polymerization process the terminal thiophene rings of TThs are bonded through α positions, generating regioregular oligomers and polymers. Moreover, during polymer doping–undoping process, electrochromism phenomenon was evidenced, extending thus the application scope of these macromolecules, e.g., in smart windows. The polymers prepared in the current work were tested in solar cells, but the results were not promising. Nevertheless, as the new synthesized monomers correspond to electron donor systems, its use in the fabrication of interpenetrating network photocells is suggested.

Acknowledgments FONDECYT financial support through project 1095165 is kindly acknowledged. IAJ and PPZ thank CONICYT for a Doctoral Scholarship.

References

1. Skotheim TA, Reynolds JR (eds) (2006) Regioregular polythiophenes. In: Conjugated polymers: theory, synthesis, properties, and characterization, 3rd edn. CRC Press, Boca Raton, pp 9.1–9.3
2. Tsekouras G, ChO Too, Wallace GG (2005) Effect of growth conditions on the photovoltaic efficiency of poly(terthiophene) based photoelectrochemical cells. Electrochim Acta 50:3224–3230. doi:10.1016/j.electacta.2004.11.053
3. Too CO, Wallace GG, Burrell AK, Collis GE, Officer DL, Boge EW, Brodie SG, Evans EJ (2001) Photovoltaic devices based on polythiophenes and substituted polythiophenes. Synth Met 123(1): 53–60. doi:10.1016/S0379-6779(00)00575-0

4. Zotti G, Marin RA, Gallazzi MC (1997) Electrochemical polymerization of mixed alkyl-alkoxybithiophenes and -terthiophenes. Substitution-driven polymerization from thiophene hexamers to long-chain polymers. Chem Mater 9(12):2945–2950. doi:10.1021/cm970295o
5. Videlot C, Fichou D (1999) Influence of molecular orientation on the photovoltaic properties of octithiophene. Synth Met 102:885–888. doi:10.1016/S0379-6779(98)00377-4
6. Zanardi Ch, Scanu R, Pigani L, Pilo MI, Sanna G, Seeber R, Spano N, Terzi F, Zucca A (2006) Synthesis and electrochemical polymerisation of 3′-functionalised terthiophenes. Electrochemical and spectroelectrochemical characterisation. Electrochim Acta 51:4859–4864. doi:10.1016/j.electacta.2006.01.025
7. Bäuerle P, Würthner F, Heid S (1990) Facile synthesis of 3-(ω-haloalkyl)thiophenes as key building blocks for functionalizated thiophenes and polythiophenes. Angew Chem Int Ed Engl 29:419–420. doi:10.1002/anie.199004191
8. Tamao K, Sumitani K, Kumada M (1972) Selective carbon–carbon bond formation by cross-coupling of Grignard reagents with organic halides. Catalysis by nickel-phosphine complexes. J Am Chem Soc 94(12):4374–4376. doi:10.1021/ja00767a075
9. Roncali J (1997) Synthetic principles for bandgap control in linear π-conjugated systems. Chem Rev 97:173–205. doi:10.1021/cr950257t
10. Jadamiec M, Lapkowski M, Matlengiewicz M, Brembilla A, Henry B, Rodehüser L (2007) Electrochemical and spectroelectrochemical evidence of dimerization and oligomerization during the polymerization of terthiophenes. Electrochim Acta 52:6146–6154. doi:10.1016/j.electacta.2007.04.011
11. Bernède JC (2008) Organic photovoltaic cells: history, principle and techniques. J Chil Chem Soc 53(3):1549–1564. doi:10.4067/S0717-97072008000300001
12. Kouskoussa B, Morsli M, Benchouk K, Louarn G, Cattin L, Khelil A, Bernède JC (2009) On the improvement of the anode/organic material interface in organic solar cells by the presence of an ultra-thin gold layer. Phys Status Solidi A 206(2):311–315. doi:10.1002/pssa.200824343
13. Ooyama Y, Harima Y (2009) Molecular designs and synthesis of organic dyes for dye-sensitized solar cells. Eur J Org Chem 18:2903–2934. doi:10.1002/ejoc.200900236
14. Cheng YJ, Yang SH, Hsu CS (2009) Synthesis of conjugated polymers for organic solar cell applications. Chem Rev 109:5868–5923. doi:10.1021/cr900182s